Understanding the Fe I Line Measurements Returned by the Helioseismic and Magnetic Imager (HMI)

D.P. Cohen[1,2] · **S. Criscuoli**[1] · **L. Farris**[1,3] · **A. Tritschler**[1]

Abstract The *Helioseismic and Magnetic Imager* (HMI) onboard the *Solar Dynamics Observatory* (SDO) observes the Sun at the Fe I 6173 Å line and returns full-disk maps of line-of-sight (LOS) observables including the magnetic flux density, velocities, Fe I line width, line depth, and continuum intensity. These data are estimated through an algorithm (the MDI-like algorithm, hereafter) that combines observables obtained at six wavelength positions within the Fe I 6173 Å line. To properly interpret such data, it is important to understand any effects of the instrument and of the pipeline that generates these data products. We tested the accuracy of the line width, line depth, and continuum intensity returned by the MDI-like algorithm using various one-dimensional (1D) atmosphere models. It was found that HMI estimates of these quantities are highly dependent on the shape of the line, therefore on the LOS angle and the magnetic flux density associated with the model, and less to line shifts with respect to the central positions of the instrument transmission profiles. In general, the relative difference between synthesized values and HMI estimates increases toward the limb and with the increase of the field; the MDI-like algorithm seems to fail in regions with fields larger than approximately 2000 G. Instrumental effects were investigated by analyzing HMI data obtained at daily intervals for a span of three years at disk center in the quiet Sun and hourly intervals for a span of 200 hours. The analysis revealed periodicities induced by the variation of the orbital velocity of the observatory with respect to the Sun, and long-term trends attributed to instrument adjustments, re-calibrations, and instrumental degradation.

✉ D.P. Cohen
danielcohen@ucla.edu

1   National Solar Observatory Sacramento Peak, P.O. Box 62, Sunspot, NM, 88349-0062, USA

2   Department of Physics and Astronomy, UCLA, Los Angeles, CA 90095-1547, USA

3   Department of Astronomy, New Mexico State University, P.O. Box 30001, 4500 Las Cruces, USA

1. Introduction

The *Helioseismic and Magnetic Imager* (HMI) onboard the *Solar Dynamics Observatory* (SDO) samples the magnetically sensitive photospheric Fe I 6173.34 Å absorption line through six narrow-band filters in right- and left-circular polarized light. Like the data-reduction pipeline of the *Michelson Doppler Interferometer* (MDI) onboard the *Solar and Heliospheric Observatory* (SOHO) (which sampled the Ni 6768 Å line at five wavelength positions), the HMI pipeline employs an algorithm (the MDI-like algorithm) that combines the filtergrams to obtain measurements of line-of-sight (LOS, hereafter) Doppler velocity, magnetic flux density, and Fe I continuum intensity. As a by-product, the MDI-like algorithm also provides estimates of the Fe I line depth and width. We refer to the continuum intensity, line depth, and width as line parameters, hereafter.

The MDI-like algorithm assumes that the profile of the observed line is Gaussian-shaped. This assumption, together with uncertainties in the transmission profiles of the instrument, saturation of the line in the presence of strong magnetic fields, and Doppler shifts induced by plasma motion and solar rotation, is known to have caused uncertainties in measurements returned by the MDI. For instance, Wachter, Schou, and Sankarasubramanian (2006), Rajaguru *et al.* (2007) and Wachter (2008) investigated uncertainties in Doppler velocity estimates. Tran *et al.* (2005), Demidov and Balthasar (2009) and Ulrich *et al.* (2009) investigated uncertainties in magnetic flux measurements, while Mathew *et al.* (2007) and Criscuoli *et al.* (2011) focused on uncertainties in continuum intensities.

Similarly, recent studies have investigated the accuracy of HMI measurements. Fleck, Couvidat, and Straus (2011) employed three-dimensional hydrodynamic simulations to study the effects of uncertainties in the shape and position of the HMI transmission profiles on Doppler velocity estimates. Liu *et al.* (2012), Pietarila *et al.* (2013) and Riley *et al.* (2014) compared HMI magnetic flux measurements with those obtained with MDI and other instruments and derived conversion factors between the various magnetograms. The analysis by Liu *et al.* (2012) showed in particular that HMI magnetic flux-density measurements are affected by 24- and 12-hour periodicities, induced by the SDO orbital motion.

Couvidat *et al.* (2012) employed high spatial resolution spectro-polarimetric observations of an active region at disk center obtained at the *Dunn Solar Telescope* with the *Interferometric Bidimensional Spectropolarimeter* (IBIS) instrument (Cavallini, 2006) to investigate the effects of line shape and velocity on all the data products (LOS velocity, magnetic flux density and Fe I line parameters) returned by the MDI-like algorithm. These authors found that the differences between measurements derived from the IBIS observations and those derived applying the MDI-like algorithm to the observed spectral profiles are in general below 20 %, with the best estimates obtained for the continuum intensity (below 2 %).

In addition to uncertainties resulting from assumptions in the derivation of the MDI-like algorithm, the HMI measurements are known to be affected by instrumental effects. These include a long-term increase of the opacity of the entrance window, variations of the focus, and uncertainties in the shape and position of the filter transmission profiles (Couvidat 2014, private communication). These effects are partially compensated for in the case of velocity and magnetic field measurements along with continuum intensity measurements, but not so for the Fe I line depth and width. Moreover, the effects of variations of instrument characteristics on the HMI data product, especially on long temporal scales (months to years) have not been presented in the literature yet.[1]

---

[1]Some information on instrument characteristics/calibrations can be found at http://jsoc.stanford.edu/.

Figure 1 Example of the six HMI transmission filter profiles. The thicker line is a synthetic Fe I 6173 Å line computed using a FAL-C (quiet-Sun) model.
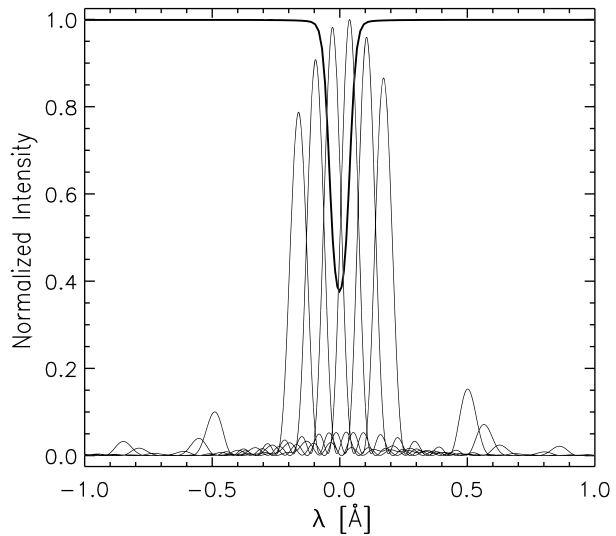
It is important to stress that the main purpose of the HMI pipeline is to provide Dopplergrams, magnetograms, and Fe I continuum intensity, while the Fe I line width and depth are a by-product of the MDI-like algorithm. For this reason, little effort has been dedicated to improving such measurements (see also Section 2). On the other hand, investigations of properties of line profiles are interesting for several types of studies, especially those in the framework of sun-as-a-star and long-term variations of solar magnetism (*e.g.*, Criscuoli *et al.*, 2013; Bertello, Pevtsov, and Pietarila, 2012; Pietarila and Livingston, 2011; Livingston *et al.*, 2007; Penza, Pietropaolo, and Livingston, 2006).

In this study we therefore investigate the accuracy of HMI data products, focusing on the Fe I line-shape parameter estimates. To this end, we employ synthetic Fe I line profiles to test the MDI-like algorithm, extending the work by Couvidat *et al.* (2012) to a larger sample of different LOS values, Doppler shift and magnetic field strength. We also employ HMI data to investigate the effects of SDO's orbital motion and instrumental degradation on short (days) and long-term (months to years) measurements of the Fe I line parameters.

The article is organized as follows: the implementation of the MDI-like algorithm is briefly described in Section 2, tests of this algorithm using synthesized line profiles are discussed in Section 3, the analysis of HMI data is presented in Section 4, and our findings and their implications are summarized in Section 5.

2. The MDI-Like Algorithm

The HMI uses a narrow-band tunable filter to sample the Fe I 6173 Å line at six different wavelength positions.

Figure 1 displays an example of the transmission profiles for each of the wavelength positions along with a synthesized iron line using a 1D quiet-Sun atmosphere model (FAL-C) (Fontenla *et al.*, 1999). As the line is sampled in both left- and right-circular polarized light (LCP and RCP, hereafter), 12 filtergrams are obtained during the wavelength-tuning process. After standard data correction (flat field, dark current, cosmic rays), these filtergrams

are used to compute derived data products (*i.e.* observables) such as Dopplergrams, magnetograms, line-width, line-depth and continuum-intensity maps employing a MDI-like algorithm. In synthesis, the algorithm estimates the data products as functions of the first two discrete Fourier coefficients of the Fe I line profile, which is assumed to be Gaussian-shaped. The Fourier coefficients are estimated by a proper combination of the filtergram intensities. A complete description of the algorithm and of its implementation is given in Couvidat *et al.* (2012). In the Appendix we only summarize the steps necessary for estimating the Fe I line parameters.

We implemented the algorithm in the Interactive Data Language (IDL). The main difference between our implementation and the one described in Couvidat *et al.* (2012) is in the HMI map employed to estimate the σ parameters used to compute the continuum intensity and line depth, as explained in the Appendix.

Estimates derived by the MDI-like algorithm are affected by uncertainties induced by the physical and numerical assumptions on which the algorithm was derived. Namely, these uncertainties are generated by deviations of the Fe I line from a Gaussian profile, the deviation of the transmission profiles from δ-functions, the assumption that a discrete Fourier transform can be computed based on only six data points, and the use of only two orders in the Fourier expansion. Moreover, changes of the shape of the transmission filter profiles, together with relative shifts of the transmission filter positions with respect to the center of the line (induced either by drifts of the transmission profiles or Doppler effects) also affect the estimates of the data products. The HMI-pipeline employs proper look-up tables to partially compensate for these effects. Nevertheless, these corrections are only applied to the Doppler velocity and magnetic field and thus partially to the Fe I continuum intensity, which is a function of the Doppler shift (see Equation (6) in the Appendix). The Fe I line depth and width estimates are a by-product of the MDI-like algorithm and no further correction is applied to them.

3. Tests on Synthetic Profiles

To investigate the effects of the deviation of the line shape from a Gaussian and the effects caused by the shift of the line with respect to the HMI wavelength filter positions, we used synthesized profiles of the Fe I 6173 Å line as an input to the MDI-like algorithm. The synthesized input profiles were computed in non-local thermodynamic equilibrium with the RH code (Uitenbroek, 2001) on a spectral range centered on a line that was 3 Å wide.

Since the shape of a spectral line is determined by the physical properties of the plasma, and, in the case of magnetically sensitive lines, by the magnetic field strength, we synthesized the line using various static one-dimensional atmosphere models representing different features observed on the solar disk. Quiet-Sun, network- and facular-region profiles were synthesized using FAL99 models (Fontenla *et al.*, 1999), while sunspot profiles were synthesized using Kurucz models characterized by various effective temperatures. We also performed tests on the three Maltby models as described in Criscuoli *et al.* (2011); the results obtained with these latter models qualitatively agree with those found from the Kurucz models and therefore they are not discussed here. To investigate the effects of the Zeeman splitting on lines, the facular model FAL-P and the sunspot models were synthesized by imposing a vertical magnetic field of constant strength. Although the imposed magnetic fields are arbitrarily associated with the model effective temperature, the values do follow the widely known anticorrelation between magnetic field and temperature in sunspots (*e.g.*, Schad, 2014, and references therein). The models employed and the corresponding magnetic

Table 1 1D atmosphere models used to synthesize the Fe I line and corresponding vertical magnetic field values (Fontenla *et al.*, 1999). The Kurucz models are denoted Kur_XXXX, where XXXX is the effective temperature in Kelvin.

Model	Description	B [kG]
FAL-A	quiet Sun	–
FAL-C	quiet Sun	–
FAL-E	faint network	–
FAL-P	facula	1.00
Kur_5500	sunspot	1.10
Kur_5250	sunspot	1.70
Kur_4750	sunspot	2.25
Kur_4500	sunspot	2.50
Kur_4250	sunspot	3.00
Kur_4000	sunspot	3.50
Kur_3750	sunspot	4.00

field strengths are summarized in Table 1. For each model we considered eight viewing angles, expressed in the following as the cosine of the heliocentric angle, μ. Note that by synthesizing the line for different viewing angles, we equivalently investigate the effect of inclined magnetic fields. Examples of line profiles generated using these models are shown in Figure 2. To investigate the effects of velocities due to convective motions, solar rotation, and relative motions between the observatory and the Sun, we also shifted the line profiles between $[-4, 4]$ km s^{-1} (note that the SDO velocity relative to the Sun spans between -3.2, and 3.2 km s^{-1}). The line parameters were estimated by feeding the synthetic profiles to the MDI-like algorithm, and the obtained values were compared with those derived from direct estimates on the synthetic profiles (synthetic values, hereafter). In particular, following the definitions of the MDI-like algorithm (see Appendix) for the line parameters, we defined the synthetic continuum as the intensity synthesized at 0.5 Å from line center, the line depth as the difference between the emerging intensities in the continuum and at the center of the line, while the line width was estimated as the full width at half maximum. All line parameters were derived separately for the LCP and RCP components of the spectral line and then averaged to give the final value.

3.1. Line-Shape Effects: Model and Line-of-Sight Dependence

Figure 3 shows the relative difference among the line parameters derived with the MDI-like algorithm and the synthetic ones for the FAL99 models and for various lines of sight. The plots show that the relative difference obtained from FAL-A, FAL-C, and FAL-E are similar and that in particular the MDI-like algorithm on these three models overestimates the line width by $5-10$ % and the line depth by $10-30$ %, with a higher relative difference in the line depth resulting at shallower lines of sight (lower μ values). Continuum intensity is found to be more accurate as the difference between synthetic values and MDI-like algorithm estimates are within 1 % with a minimum of about 0.1 % close to disk center. The differences obtained with the FAL-P model representative of a facular region with a vertical magnetic field of 1000 G, are larger and have opposite sign with respect to the other FAL models investigated. This is because the Fe I line-shape profiles obtained from the first three models are similar and close to the shape of a Gaussian profile, whereas the shape obtained from the FAL-P is broadened by the Zeeman effect (as shown in Figure 2). The line width is in fact underestimated by $15-20$ %, the line depth is overestimated by $20-60$ %, and the continuum intensity is underestimated by $0.5-2$ %. The differences for this model decrease
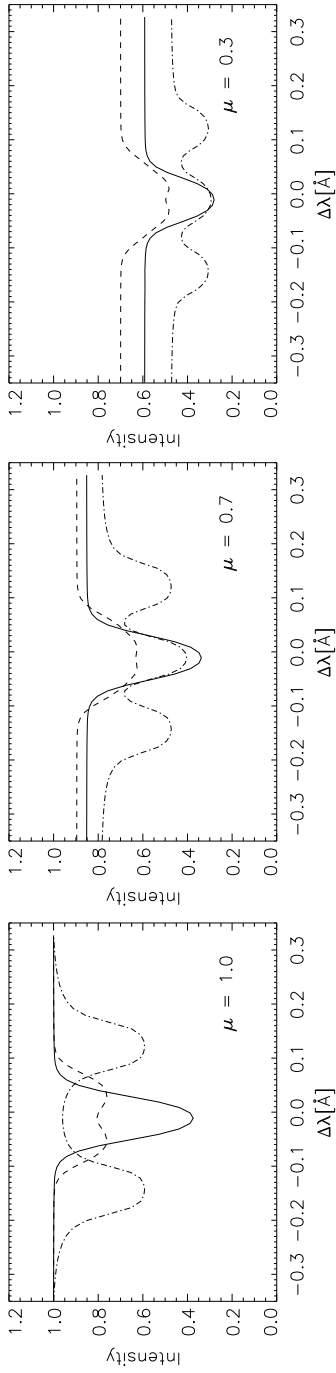
Figure 2 Examples of Fe I line profiles synthesized through three 1D atmosphere models at three viewing angles. Continuous line: FAL-C. Dashed line: FAL-P with uniform magnetic field of 1000 G. Dotted-dashed line: Kurucz_4250 with uniform magnetic field of 3000 G. All profiles have been normalized to the corresponding continuum intensity at disk center.
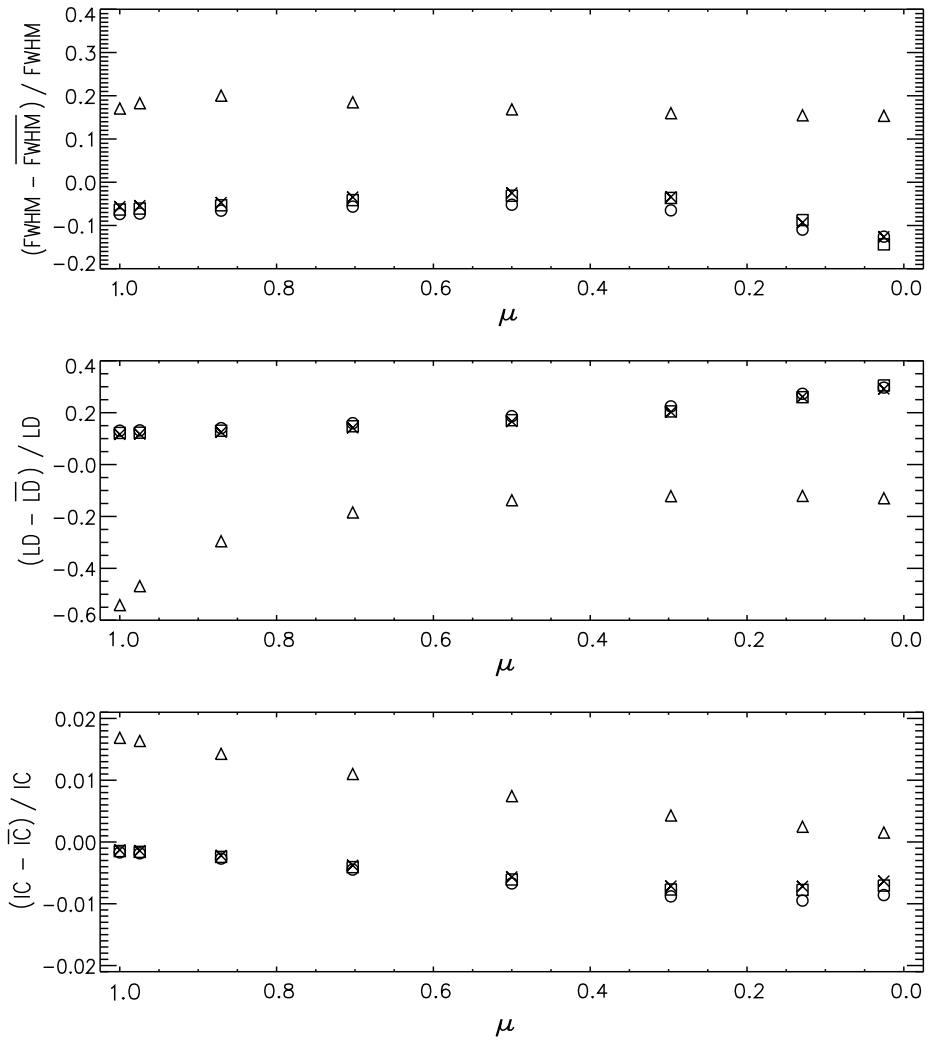
Figure 3 Relative differences between synthetic and MDI-like algorithm-calculated line parameter values for the FAL99 models: FAL-A (open circle), FAL-C (open square), FAL-E (X), and FAL-P (open triangle). FWHM denotes the line-width, LD the line depth, and IC the continuum intensity. The bar on top of the acronyms denotes quantities returned by the MDI-like algorithm.

toward the limb, because, as shown in Figure 2, the line-core intensity enhancement due to the Zeeman splitting decreases for shallower LOS.

The results obtained for all seven Kurucz models are plotted in Figure 4. The relative difference between the synthetic values and those returned by the MDI-like algorithm are very large, with the lowest values found for the continuum intensity, for which the discrepancy is up to 20 %. For the line depth and the line width the differences are up to 100 %. In general, the differences increase with the increase of the magnetic field strength as a consequence of both the line saturation and the poor sampling of the wings and continuum in the case of large line broadening. In particular, for magnetic field intensities higher than approximately
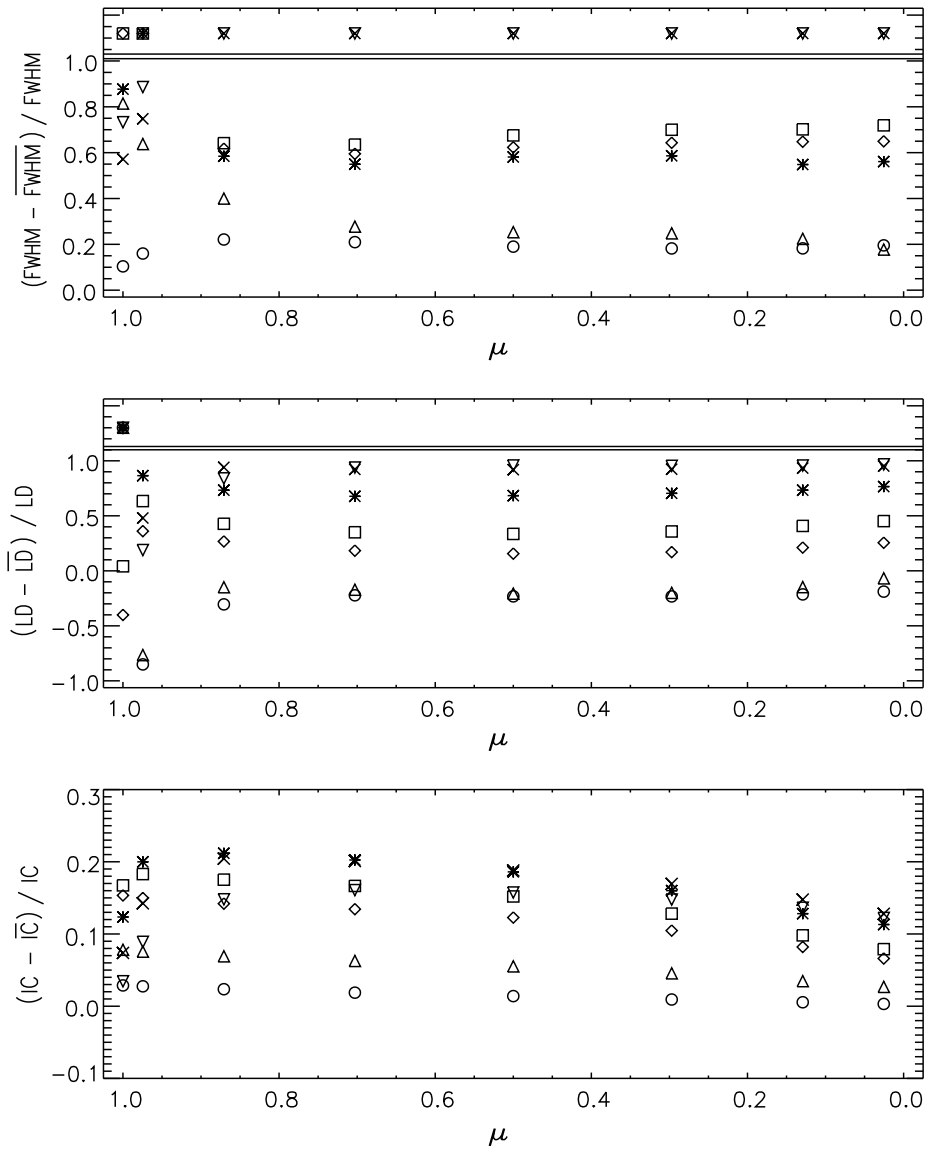
Figure 4 Relative differences between theoretical and MDI-like algorithm-calculated line-shape values for the Kurucz sunspot models: Kur_5500 (open circle), Kur_5250 (open upward triangle), Kur_4750 (open diamond), Kur_4500 (open square), Kur_4250 (star), Kur_4000 ('X'), and Kur_3750 (open downward triangle). FWHM denotes the line-width, LD the line depth, and IC the continuum intensity. The bar on top of the acronyms denotes quantities returned by the MDI-like algorithm.

2000 G, the MDI-like algorithm returned unphysical line-width estimates. These cases are marked above the double line in the plots. This occurs because for these models the sum of the squares of the second Fourier coefficients is greater than the sum of the squares of the first Fourier coefficients, so that the argument of the logarithm in Equation (4) in the Appendix returns a negative number whose square root is not real. Similarly, the 'infinite'

relative difference found at vertical lines of sight for the line depth (these cases are also beyond the double line in the plot) are due to the saturation of the line at large magnetic field strengths (see Figure 2), so that the synthetic line depth tends to zero, while the MDI-like algorithm, expecting a Gaussian-shaped profile, returns a higher value. It is also interesting to note that for the largest magnetic field strengths investigated, the deviations from the synthetic values of the line depth and of the line width present small center-to-limb variation because of saturation effects. For the same reason, as already pointed out in previous studies investigating the accuracy of the MDI algorithm (Mathew *et al.*, 2007; Criscuoli *et al.*, 2011), the discrepancies of the continuum intensities do not increase monotonically with the increase of the magnetic field strength, instead, they decrease for the highest field values investigated.

3.2. Line-Shift Effects

We also investigated the influence of a line shift on the determination of the line parameters. In the following we only report results obtained with the FAL99 models because those obtained for sunspots agree qualitatively. Figure 5 shows the relative difference between the values obtained from the MDI-like algorithm with the line at rest and the line shifted *versus* the amount of shift. The plots reveal a periodicity for all the line parameters, which is proportional to the spacing between the HMI transmission profiles (see also Wachter, 2008; Criscuoli *et al.*, 2011).

The variations obtained for models FAL-A, -C, and -E are similar in amplitude (a few percent) and sign, whereas the results obtained with the FAL-P model show larger deviations (up to 13 %) and opposite sign, in agreement with the results presented in Figure 3. The increase of the difference between measured and synthetic values is due in this case to the fact that a line shift causes the left and right wings of the line to be unevenly sampled. The broadening induced by the Zeeman splitting enhances this effect (for larger broadenings even modest shifts may cause portions of one of the wings not to be sampled at all), so that it is no surprise that the uncertainties increase with the increase of the magnetic field strength associated with the model.

In agreement with results presented in Criscuoli *et al.* (2011) for the continuum intensity estimated by the MDI algorithm, the plots also show asymmetries around zero velocity. Criscuoli *et al.* (2011) ascribed this to the fact that a line shift could compensate for or enhance the original shift of the lines that they employed (obtained from nonstatic simulations and observations) for their tests. Because the results presented in Figure 5 have been obtained with static models, the asymmetries around the zero velocity must be ascribed to small asymmetries in the filter transmission profiles.

Finally, it is worth to note that the results reported in Figure 5 allow addressing effects introduced only by line shifts. In practice, uncertainties are introduced by the combined effect of line shape and line shift. For each model and shift, it is easy to show that if h is the uncertainty resulting from the deviation of the line shape from a Gaussian profile (results reported in Figure 3) and h' is the uncertainty resulting from a line shift (results reported in Figure 5), then the uncertainty resulting by the combination of the two effects is $h + h' + h \cdot h'$.

4. Tests on HMI Data

The results presented in the previous section indicate that the accuracy with which the MDI-like algorithm estimates the Fe I line parameters strongly depends on the shape of the line
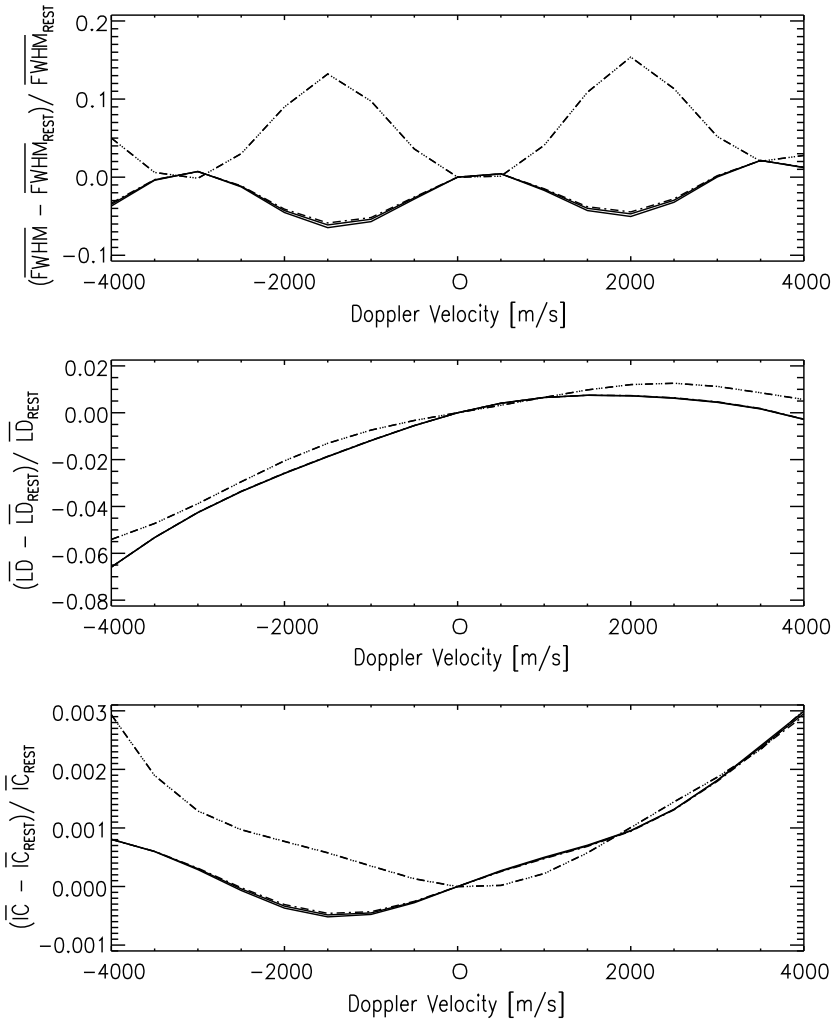
Figure 5 Relative differences of line parameters calculated with the MDI-like algorithm between Doppler-shifted line and line at rest for the Fe I line generated by the Fontenla models at $\mu = 1$. Solid line: FAL-A. Dashed line: FAL-C. Dotted–dashed line: FAL-E. Triple-dotted–dashed line: FAL-P.

profiles and the line shift. The first effect dominates, at least for shifts in the range investigated. We expect studies aiming at investigating the center-to-limb variation or the temporal evolution of magnetic features to be particularly affected. For instance, Liu *et al.* (2012) showed that the evolution of the LOS magnetic flux density of an active region (AR) measured by HMI presents 12- and 24-hour cyclic variations that are generated by the orbital motion of the SDO. This signal is superimposed on a longer temporal trend resulting from the combination of the change of the LOS with solar rotation Doppler effects as the region crosses the solar disk. To investigate these effects also on the line-shape parameters returned by the HMI, we repeated the analysis performed by Liu *et al.* (2012) on a different region (*i.e.* AR 11092) and investigated the evolution of the line parameters and of the magnetic flux density on quiet, facular, and sunspot regions.
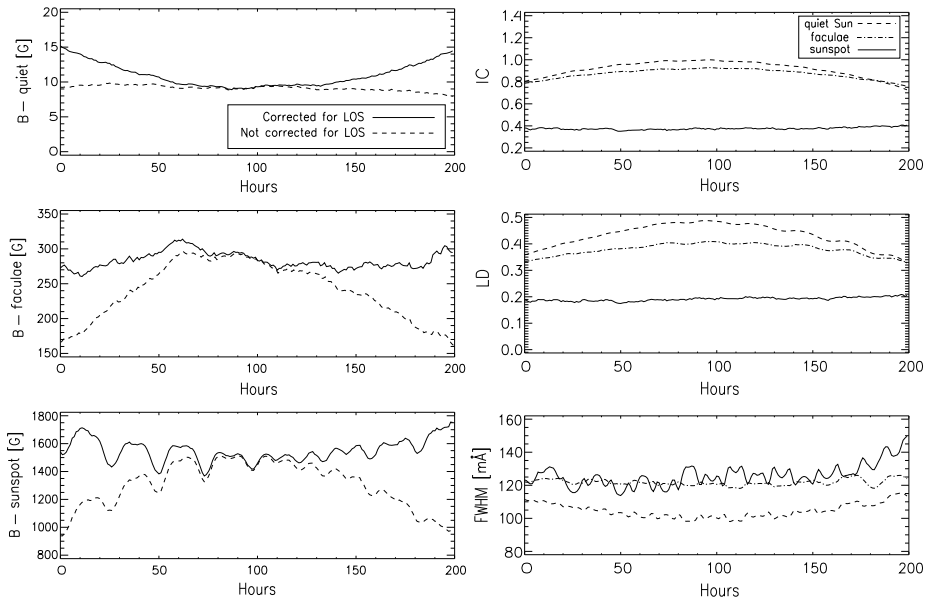
Figure 6 Variation of average magnetic flux density (left) and average line-shape parameters (right) of quiet, facular, and sunspot pixels (see text) observed around AR11092 by the HMI. The observations started on July 30, 2010 at 11:58:26 UT. The region was at the closest proximity to disk center about 100 hours after the beginning of the observations. Continuum intensity and line depth are normalized to the average continuum intensity of quiet pixels at disk center.

We also analyzed the variation of the line-shape parameters over a data set of HMI observations spanning about three years with the aim to investigate the effects of instrumental degradation described in Section 1. As properties of magnetic features can vary over the cycle, for this last analysis only quiet-Sun regions at disk center were considered.

4.1. Short-Term Line Parameter Variations

To investigate short-term effects of solar rotation and orbital velocities on HMI data products, we analyzed a one-hour-cadence data set spanning about 200 hours in total, acquired between July 30 and August 8, 2010. In particular, we analyzed the 720-second magnetic flux, line-depth, continuum intensity, and line-width data products. We employed magnetograms corrected for the foreshortening ($B = B_{obs}/\mu$) to identify quiet (pixels where the absolute magnetic flux density is ≤ 100 G), facular (pixels where the absolute magnetic flux density is > 100 and ≤ 1000 G) and sunspot (pixels where the absolute magnetic flux density is > 1000 G) regions around AR 11092 (NOAA number). This active region was chosen because it showed little evolution during its passage over the disk. For each class of pixels we then studied the temporal variation of the average Fe I line parameters and the magnetic flux density. The investigation of the average magnetic flux density allowed verifying that the observed line parameter variations were not caused by the evolution of the magnetic field in the region. The variations of the average magnetic flux density computed over the three classes of regions are reported in Figure 6 (left panel). The dashed and continuous lines represent the magnetic flux density uncorrected and corrected for the foreshortening, respectively. These plots agree with results reported in Liu *et al.* (2012), who showed that

the magnetic flux density of an active region uncorrected for the foreshortening is highest at disk center, while the flux density of quiet regions does not depend on the position on the disk. When correcting for the foreshortening, the curves change concavity, with a minimum observed at disk center, suggesting that the trends reported in Liu *et al.* (2012) are mostly caused by projection effects. Semidiurnal and diurnal periodic variations of the flux are also observed. These, as explained in Liu *et al.* (2012), can be mostly ascribed to spacecraft orbital motion effects not entirely compensated for by the look-up tables. The mostly symmetric trends around disk center suggest that the magnetic field of the region stayed fairly constant during the observation time.

The right panel in Figure 6 shows results obtained for the line parameters. The plots show that like the magnetic flux density, line parameters are symmetric around the time of closest proximity to disk center. These variations must be mostly ascribed to the combination of LOS effects and solar rotation. The typical periodicities caused by orbital motions of the satellite are also observed. These are more noticeable for the line width in magnetized pixels, as expected from the results discussed in Section 3.2. It is important to note that all the observed temporal variations are due to both LOS and velocity effects and that it is not possible, in practice, to distinguish between them. However, a comparison of the results presented in Sections 3.1 and 3.2 suggests that the long-term trends of the continuum intensity and line depth reported in Figure 6 are mostly caused by LOS effects and not by the solar rotation, because variations induced by this last effect (the solar rotation is $\pm 2 \, \mathrm{km \, s^{-1}}$ at the equator) are about one order of magnitude smaller than variations induced by LOS effects. As a consequence, the line parameters show almost no variation in sunspot pixels because, as shown in Section 3.1, the shape of a line in highly magnetized regions is dominated by the Zeeman splitting, not by LOS effects.

4.2. Long-Term Line Parameter Variations

To investigate long-term variations of the Fe I line parameters returned by the HMI, we have analyzed a set of magnetic flux density, line-depth, continuum intensity, and line-width data acquired daily between May 1, 2010 and May 30, 2013. For this analysis we also employed 720-second data, obtained as close as possible to 12:00 UT. To facilitate distinguishing between effects inherent to the measurements from those induced by variations of magnetic feature properties induced by the solar magnetic cycle, we restricted the analysis to quiet pixels located close to disk center. To this end, we analyzed the temporal variation of the average value of the Fe I data products computed over pixels where the absolute magnetic flux density is ≤ 100 G, located in a square area of 500×500 pixels (about 250×250 arcsec) around disk center. The results are shown in Figure 7. The line-shape parameter values have been normalized to the value measured on the first day analyzed. The plots of line-shape parameters show an overall decrease with time and several discontinuities. The long-term trends are caused by various issues mentioned in Section 1 that are known to affect the HMI, such as an increase of the opacity of the entrance window (most likely induced by exposure to UV radiation), changes in the shape and positions of the transmission profiles, and variations of the focus caused by temperature changes in the entrance window especially after eclipse periods. The discontinuities are due to periodic recalibrations of the instrument that are meant to mitigate these effects. The recalibrations include an increase of the standard exposure time, retuning of the transmission profiles (the days of the retuning are marked with arrows in the figure), adjustments of the focus, and front window reheating after eclipse periods (calibrations calendar and descriptions are available at http://jsoc.stanford.edu/doc/data/hmi/). Of these effects, the increase of the entrance window opacity and the shift of the transmission
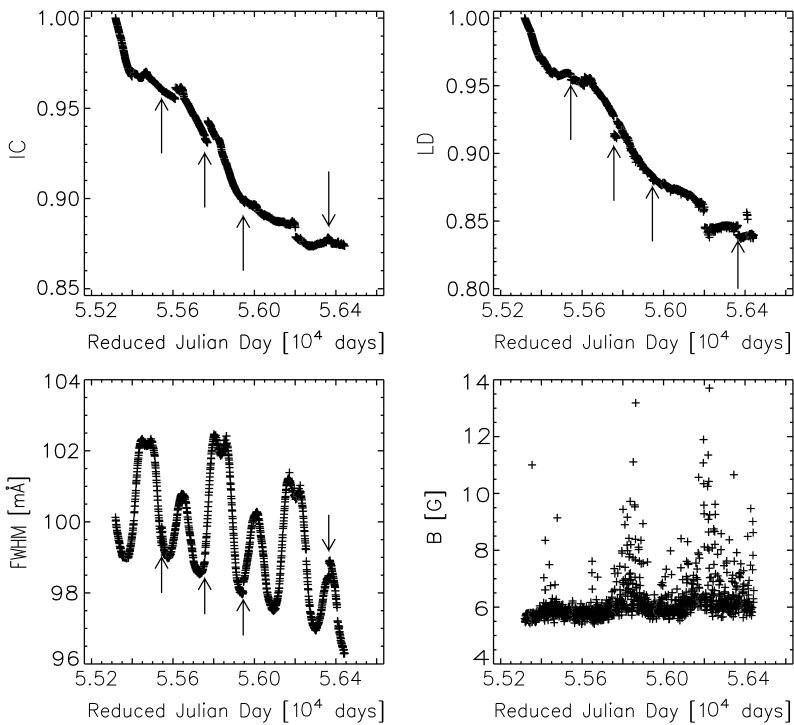
Figure 7 Line parameters and average absolute magnetic flux density observed by the HMI in quiet pixels close to disk center over a period of three years. The arrows indicate the days on which the HMI filters were retuned.

profiles dominate the long-term trends. Comparison of plots in Figures 7 and 5 indicates that the continuum intensity and line depth are mostly affected by the increase of the entrance window opacity, not by a shift of the transmission profiles. The observed long-term decrease of these quantities is in fact about 10 %. Plots in Figure 5 show that for the line depth such variation can be generated by shifts larger than about 4 km s^{-1} (which seems an improbably high value, considering that as stated above, the transmission profiles are periodically retuned), while the continuum intensity is almost insensitive to relative shifts of the line with respect to the positions of the transmission profiles. Instead, Equation (4) in the Appendix indicates that the line width is insensitive to intensity variations as long as these variations are the same for all the six filtergrams. The observed decrease of about 4 % for this parameter is compatible with shifts of the transmission profiles smaller than 1 km s^{-1}.

It is also noteworthy that the observed variations of the line parameters cannot be ascribed to variations of the quiet-Sun magnetic field. In fact, Figure 7 shows that the average absolute magnetic flux density slightly increases with time, which would cause both the line width and depth to increase. Note also that as mentioned above, the magnetic flux-density measurements are compensated for line shift effects (induced by both LOS orbital velocity changes and drifts of the transmission profiles) and that the magnetic flux density is independent of the absolute intensity of the filtergrams (see Couvidat *et al.*, 2012), so that the small flux-density increase over time, in agreement with the increase of the magnetic activity during the period analyzed, could be real.

Finally, the plots in Figure 7 show periodic variations of the line parameters that are particularly noticeable for the line width. A comparison of the Fourier spectra of the SDO velocities and of the line width (not shown) confirmed that even these oscillations are due to the relative variation of the SDO orbital velocity with respect to the Sun.

5. Discussion and Conclusions

We investigated the accuracy of the Fe I 6173 Å line-parameter values (*i.e.* line depth, line width, continuum intensity) returned by the HMI. To this aim, we first tested the accuracy of estimates returned by the MDI-like algorithm, which is part of the HMI data reduction pipeline. We then identified systematic and instrumental effects by studying the temporal evolution of HMI data obtained at different cadences over short (days) and long (years) temporal ranges.

An MDI-like algorithm was implemented and tested with synthetic Fe I 6173 Å line pro-files generated using 1D atmosphere models representing quiet-Sun, faint network, facular, and sunspot regions at different viewing angles across the solar disk. We found that the ac-curacy of this algorithm strongly depends on the line shape determined by magnetic field strength and viewing angle. The algorithm works relatively well in quiet and facular regions, where the accuracy of the continuum intensity is better than 2 % and the accuracy of the line depth and line width are on average on the order of or below 20 %. The accuracy decreases with the increase of the magnetic field strength, so that in highly magnetized regions (*e.g.* sunspots) it is in general on the order of several tens of percent, with the best accuracy found again for the continuum intensity (about or below 20 %). For a magnetic field strength larger than about 2000 G, the algorithm encounters numerical problems due to the saturation of the line, so that in these regions HMI results cannot be considered reliable. These results par-tially agree with those obtained by Couvidat *et al.* (2012), who employed observed spectra to investigate the accuracy of the data products returned by the MDI-like algorithm. In particu-lar, the accuracies that we estimated for the continuum intensity along vertical lines of sight agree well with those presented by these authors. For line width and depth, the agreement is still good in quiet and facular regions, but in regions of stronger magnetic field we obtained a lower accuracy than the one reported by Couvidat *et al.* (2012). The discrepancy between our results and those presented by these authors has to be ascribed in part to uncertainties in the radiative synthesis and assumptions in our models (*e.g.* the atomic transitions values employed, the arbitrary association of an atmosphere model with a magnetic field strength, the assumption of a vertical constant field, and the exclusion of molecules in umbra models). On the other hand, Couvidat *et al.* (2012) estimated a better accuracy in highly magnetized regions because they employed observed spectra on which the line-shape variations induced by the Zeeman splitting (especially the increase of the core intensity) are strongly reduced in amplitude by scattered light (both spatial and spectral) and finite spectral resolution effects (see also the discussion in Criscuoli *et al.*, 2011).

The effects of the line shift with respect to the nominal wavelength position of the filter transmission profiles have also been investigated, and they were in general weaker than LOS and magnetic field effects, at least for shifts in the range $[-4, 4]$ km s^{-1}.

Along with testing the HMI pipeline, we studied the Fe I line width, line depth, and continuum intensity HMI data generated at hourly intervals over a span of 200 hours in an active region and at daily intervals for a span of three years in quiet regions at disk center. We found both short-term and long-term periodicities caused by the orbit of the SDO, long-term decrease in intensity measurements due to opacity of the front window

increasing, long-term decrease in line width due to drift in wavelength of transmission filters, along with discontinuities present in the long-term data due to instrument adjustments and recalibrations. The LOS magnetic field and the LOS Doppler velocity are partially corrected for such effect, while the Fe I line parameters data are not. This complicates the analysis of temporal variations of the iron line parameters.

Thus, the Fe I line parameter estimates returned by the HMI are affected by uncertainties due to approximations on which the MDI-like algorithm works (mainly, the assumption that the line is Gaussian shaped) and to instrumental effects. These uncertainties could be reduced with the use of proper look-up tables, like those employed to correct LOS magnetic field and velocity estimates and thus continuum intensity measurements. However, such multidimensional look-up tables would probably be quite difficult to implement. Alternatively, the algorithm might benefit from being modified so as to fit the actual Fe I line profile instead of assuming a Gaussian (Couvidat *et al.*, 2012). In this case, the speed of the fitting algorithm would be a decisive measure of its utility because it would require fitting a very large number of pixels. The long-term effects induced by instrumental degradation, especially those induced by the increased opacity of the entrance window, are more difficult to correct for. It is possible to make these corrections if it is assumed that the quiet Sun does not vary, perhaps committing a small error, but long-term studies of the quiet Sun would be comprised. Because such corrections are not available yet, the results presented in this study are important for correctly interpreting the Fe I 6173 Å line-parameter estimates returned by the HMI.

Appendix: The MDI-Like Algorithm

We implemented the MDI-like algorithm following the description in Couvidat *et al.* (2012). Here we summarize only the steps necessary to estimate the Fe I line parameters.

The algorithm assumes a Gaussian-shaped Fe I line profile:

$$I(\lambda) = I_c - I_d \exp\left[-\frac{(\lambda - \lambda_0)^2}{\sigma^2}\right], \tag{1}$$

where I_c is the continuum intensity, I_d is the line depth, and σ is a parameter that defines the width. Note that the algorithm returns as an estimate of the line width, the full width at half maximum (FWHM), which is proportional to σ through the relation FWHM $= 2\sqrt{2\ln(2)}\sigma$.

The algorithm first computes discrete approximations to the first and second Fourier coefficients using the six filtergram intensities I_j:

$$a_1 \approx \frac{2}{6}\sum_{j=0}^{5} I_j \cos\left(2\pi\frac{2.5-j}{6}\right), \qquad b_1 \approx \frac{2}{6}\sum_{j=0}^{5} I_j \sin\left(2\pi\frac{2.5-j}{6}\right), \tag{2}$$

$$a_2 \approx \frac{2}{6}\sum_{j=0}^{5} I_j \cos\left(4\pi\frac{2.5-j}{6}\right), \qquad b_2 \approx \frac{4}{6}\sum_{j=0}^{5} I_j \sin\left(4\pi\frac{2.5-j}{6}\right). \tag{3}$$

In our implementation the filtergram intensities were calculated as the convolution of the synthetic iron line with each of the six transmission filter profiles. The line amplitude and depth and the continuum intensity are then calculated according to the formulas

$$\sigma = \frac{T}{\pi\sqrt{6}}\sqrt{\ln\left(\frac{a_1^2 + b_1^2}{a_2^2 + b_2^2}\right)}, \tag{4}$$

$$I_d = \frac{T}{2\sigma\sqrt{\pi}}\sqrt{a_1^2 + b_1^2}\exp\left(\frac{\pi^2\sigma^2}{T^2}\right), \tag{5}$$

$$I_c = \frac{1}{6}\sum_{j=0}^{5} I_j + I_d \exp\left[-\frac{(\lambda_j - \lambda_0)^2}{\sigma^2}\right]. \tag{6}$$

Here $T = 412.8$ mÅ is six times the nominal wavelength separation between the filter transmission profiles and λ_j corresponds to the central wavelength of the jth filter.

The actual implementation of the MDI-like algorithm is slightly different than explained above. Tests performed on Gaussian profiles have shown that the line parameters calculated using the formulas above are affected by inaccuracies generated by the finite-term Fourier expansion (using only six wavelengths to calculate the Fourier transform), the finite sampling of the line, and the fact that the transmission profiles are not δ-functions. In particular, Couvidat *et al.* (2012) reported that Equation (4) overestimates the real width by $\sim 20\%$ and that Equation (5) underestimates the actual depth by $\sim 33\%$. To take into account these uncertainties, in the actual implementation Equation (4) is multiplied by a factor of 5/6 and Equation (5) is multiplied by a factor of 6/5. Tests have also revealed that the error in the continuum intensity is only $\sim 1\%$ so that no correction factor is applied to Equation (6).

Moreover, Equations (5) and (6) are not computed using the σ values returned by Equation (4). The reason is that as shown in previous sections, the σ returned by Equation (4) suffers from uncertainties induced by strong deviations of the line shape from a Gaussian profile (like in presence of strong fields), which would cause uncertainties in the estimate of the other two line parameters. Instead, the algorithm uses standard values of σ derived from a HMI full-disk line-width map observed in a day of low activity. After the line width

Figure 8 Line-of-sight dependence of the σ values employed to compute the line depth and the continuum intensity. The x-axis is the viewing angle $\mu = \cos\theta$ and the dashed line is a fifth-order polynomial fit to the data.
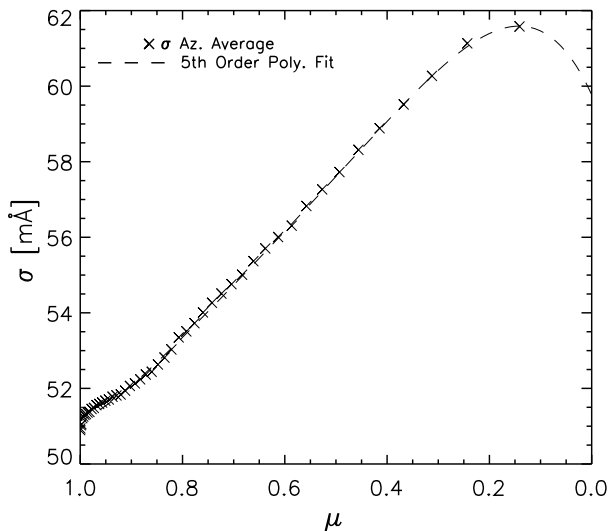
is converted into σ, the standard σ values are computed as the fifth-order polynomial fit to the variation of the azimuthally-averaged σ values with radial distance from disk center.

The values of σ as function of the cosine of the heliocentric angle employed in our implementation are illustrated in Figure 8 and were obtained from an HMI line-width map taken on September 10, 2009.

References

Bertello, L., Pevtsov, A.A., Pietarila, A.: 2012, Signature of differential rotation in Sun-as-a-Star Ca II K measurements. *Astrophys. J.* **761**, 11. DOI. ADS.

Cavallini, F.: 2006, IBIS: a new post-focus instrument for solar imaging spectroscopy. *Solar Phys.* **236**, 415. DOI. ADS.

Couvidat, S., Rajaguru, S.P., Wachter, R., Sankarasubramanian, K., Schou, J., Scherrer, P.H.: 2012, Line-of-sight observables algorithms for the Helioseismic and Magnetic Imager (HMI) instrument tested with Interferometric Bidimensional Spectrometer (IBIS) observations. *Solar Phys.* **278**, 217. DOI. ADS.

Criscuoli, S., Ermolli, I., Del Moro, D., Giorgi, F., Tritschler, A., Uitenbroek, H., Vitas, N.: 2011, Line shape effects on intensity measurements of solar features: brightness correction to SOHO MDI continuum images. *Astrophys. J.* **728**, 92. DOI. ADS.

Criscuoli, S., Ermolli, I., Uitenbroek, H., Giorgi, F.: 2013, Effects of unresolved magnetic field on Fe I 617.3 and 630.2 nm line shapes. *Astrophys. J.* **763**, 144. DOI. ADS.

Demidov, M.L., Balthasar, H.: 2009, Spectro-polarimetric observations of solar magnetic fields and the SOHO/MDI calibration issue. *Solar Phys.* **260**, 261. DOI. ADS.

Fleck, B., Couvidat, S., Straus, T.: 2011, On the formation height of the SDO/HMI Fe 6173 Å Doppler signal. *Solar Phys.* **271**, 27. DOI. ADS.

Fontenla, J., White, O.R., Fox, P.A., Avrett, E.H., Kurucz, R.L.: 1999, Calculation of solar irradiances. I. Synthesis of the solar spectrum. *Astrophys. J.* **518**, 480. DOI. ADS.

Liu, Y., Hoeksema, J.T., Scherrer, P.H., Schou, J., Couvidat, S., Bush, R.I., Duvall, T.L., Hayashi, K., Sun, X., Zhao, X.: 2012, Comparison of line-of-sight magnetograms taken by the solar dynamics Observatory/Helioseismic and magnetic imager and solar and heliospheric Observatory/Michelson Doppler imager. *Solar Phys.* **279**, 295. DOI. ADS.

Livingston, W., Wallace, L., White, O.R., Giampapa, M.S.: 2007, Sun-as-a-Star spectrum variations 1974-2006. *Astrophys. J.* **657**, 1137. DOI. ADS.

Mathew, S.K., Martínez Pillet, V., Solanki, S.K., Krivova, N.A.: 2007, Properties of sunspots in cycle 23. I. Dependence of brightness on sunspot size and cycle phase. *Astron. Astrophys.* **465**, 291. DOI. ADS.

Penza, V., Pietropaolo, E., Livingston, W.: 2006, Modeling the cyclic modulation of photospheric lines. *Astron. Astrophys.* **454**, 349. DOI. ADS.

Pietarila, A., Livingston, W.: 2011, Solar cycle variation in Sun-as-a-Star Ca II 854.2 nm bisectors. *Astrophys. J.* **736**, 114. DOI. ADS.

Pietarila, A., Bertello, L., Harvey, J.W., Pevtsov, A.A.: 2013, Comparison of ground-based and space-based longitudinal magnetograms. *Solar Phys.* **282**, 91. DOI. ADS.

Rajaguru, S.P., Sankarasubramanian, K., Wachter, R., Scherrer, P.H.: 2007, Radiative transfer effects on Doppler measurements as sources of surface effects in sunspot seismology. *Astrophys. J. Lett.* **654**, L175. DOI. ADS.

Riley, P., Ben-Nun, M., Linker, J.A., Mikic, Z., Svalgaard, L., Harvey, J., Bertello, L., Hoeksema, T., Liu, Y., Ulrich, R.: 2014, A multi-observatory inter-comparison of line-of-sight synoptic solar magnetograms. *Solar Phys.* **289**, 769. DOI. ADS.

Schad, T.A.: 2014, On the collective magnetic field strength and vector structure of dark umbral cores measured by the Hinode spectropolarimeter. *Solar Phys.* **289**, 1477. DOI. ADS.

Tran, T., Bertello, L., Ulrich, R.K., Evans, S.: 2005, Magnetic fields from SOHO MDI converted to the mount Wilson 150 foot solar tower scale. *Astrophys. J. Suppl. Ser.* **156**, 295. DOI. ADS.

Uitenbroek, H.: 2001, Multilevel radiative transfer with partial frequency redistribution. *Astrophys. J.* **557**, 389. DOI. ADS.

Ulrich, R.K., Bertello, L., Boyden, J.E., Webster, L.: 2009, Interpretation of solar magnetic field strength observations. *Solar Phys.* **255**, 53. DOI. ADS.

Wachter, R.: 2008, Instrumental response function for filtergraph instruments. *Solar Phys.* **251**, 491. DOI. ADS.

Wachter, R., Schou, J., Sankarasubramanian, K.: 2006, Line shape changes and Doppler measurements in solar active regions. I. A method for correcting Dopplergrams from SOHO MDI. *Astrophys. J.* **648**, 1256. DOI. ADS.